Research Article | Vol. 6, No. 10 | 1 Oct 2016 | OPTICAL MATERIALS EXPRESS 3293

Optical Materials EXPRESS

Enhanced light extraction in wafer-bonded *p*-side-up thin-film AlGaInP light emitting diodes via zinc oxide nanorods

MING-CHUN TSENG,[1] DONG-SING WUU,[1,2] CHI-LU CHEN,[3] HSIN-YING LEE,[4] YU-CHANG LIN,[4] AND RAY-HUA HORNG[2,5,*]

[1]*Department of Materials Science and Engineering, National Chung Hsing University, Taichung 402, Taiwan*
[2]*Advanced Optoelectronic Technology Center, National Cheng Kung University, Tainan 701, Taiwan*
[3]*Graduate Institute of Precision Engineering, National Chung Hsing University, Taichung 402, Taiwan*
[4]*Department of Photonics, National Cheng Kung University, Tainan 701, Taiwan*
[5]*Department of Electronics Engineering, National Chiao Tung University, Hsinchu 300, Taiwan*
[*] *rhh@nctu.edu.tw*

Abstract: ZnO nanorods grown via hydrothermal method on the aluminum-doped zinc oxide (AZO) thin film were used to fabricate high-brightness *p*-side-up thin-film AlGaInP light-emitting diodes (LEDs). The AZO thin film was not only used as current spreading layers but also as a seed layer of ZnO nanorods. The AZO thin film was prepared using atomic layer deposition. The ZnO nanorods improved light extraction, thus increasing the light output power of the LEDs. The output powers of LEDs with optimum ZnO nanorod structures were increased by 32% at an injection current of 700 mA, as compared with that of an LED with AZO thin film. The emission wavelength shifts of LEDs with an AZO thin film and optimum ZnO nanorod structure were 18 and 11 nm, respectively, when the injection current was increased from 20 to 1000 mA. The ZnO nanorods not only provide more light extraction but also keep the thermal stability of the LED device without any degradation. The results are promising for the developed high brightness AlGaInP LED applications with low fabrication cost through ZnO nanorods grown by hydrothermal method to enhance the light extraction efficiency.

OCIS codes: (230.0230) Optical devices; (230.3670) Light-emitting diodes.

References and links

1. E. F. Schubert and J. K. Kim, "Solid-state light sources getting smart," Science **308**(5726), 1274–1278 (2005).
2. E. F. Schubert, *Light-Emitting Diodes,* 2nd ed. (Cambridge University Press, 2006), chap. 5.
3. M. R. Krames, M. Ochiai-Holcomb, G. E. Höfler, C. Carter-Coman, E. I. Chen, I. H. Tan, P. Grillot, N. F. Gardner, H. C. Chui, J. W. Huang, S. A. Stockman, F. A. Kish, M. G. Craford, T. S. Tan, C. P. Kocot, M. Hueschen, J. Posselt, B. Loh, G. Sasser, and D. Collins, "High-power truncated inverted pyramid $Al_xGa_{1-x})_{0.5}In_{0.5}P$/GaP light-emitting diodes exhibiting >50% external quantum efficiency," Appl. Phys. Lett. **75**(16), 2365–2367 (1999).
4. R. Windisch, B. Dutta, M. Kuijk, A. Knobloch, S. Meinlschmidt, S. Schoberth, P. Kiesel, G. Borghs, G. H. Döhler, and P. Heremans, "40% efficient thin film surface textured light emitting diodes by optimization of natural lithography," IEEE Trans. Electron Dev. **47**(7), 1492–1498 (2000).
5. T. Kim, P. O. Leisher, A. J. Danner, R. Wirth, K. Streubel, and K. D. Choquette, "Photonic crystal structure effect on the enhancement in the external quantum efficiency of a red LED," IEEE Photonics Technol. Lett. **18**(17), 1876–1878 (2006).
6. M. C. Tseng, C. L. Chen, N. K. Lai, S. I. Chen, T. C. Hsu, Y. R. Peng, and R. H. Horng, "P-side-up thin-film AlGaInP-based light emitting diodes with direct ohmic contact of an ITO layer with a GaP window layer," Opt. Express **22**(S7), A1862–A1867 (2014).
7. R. H. Horng, B. R. Wu, C. F. Weng, P. Ravadgar, T. M. Wu, S. P. Wang, J. H. He, T. H. Yang, Y. M. Chen, T. C. Hsu, A. S. Liu, and D. S. Wuu, "P-side up AlGaInP-based light emitting diodes with dot-patterned GaAs contact layers," Opt. Express **21**(17), 19668–19674 (2013).
8. R. H. Horng, C. E. Lee, C. Y. Kung, S. H. Huang, and D. S. Wuu, "High-power AlGaInP light-emitting diodes with patterned copper substrates by electroplating," Jpn. J. Appl. Phys. **43**(4B), L576–L578 (2004).
9. H. K. Lee, M. S. Kim, and J. S. Yu, "Light-extraction enhancement of large-area GaN-based LEDs with electrochemically grown ZnO nanorod arrays," IEEE Photonics Technol. Lett. **23**(17), 1204–1206 (2011).

#273044 http://dx.doi.org/10.1364/OME.6.003293
Journal © 2016 Received 2 Aug 2016; revised 20 Sep 2016; accepted 22 Sep 2016; published 27 Sep 2016

Optical Materials EXPRESS

10. Z. Yin, X. Liu, Y. Wu, X. Hao, and X. Xu, "Enhancement of light extraction in GaN-based light-emitting diodes using rough beveled ZnO nanocone arrays," Opt. Express **20**(2), 1013–1021 (2012).
11. M. Ma, F. W. Mont, X. Yan, J. Cho, E. F. Schubert, G. B. Kim, and C. Sone, "Effects of the refractive index of the encapsulant on the light-extraction efficiency of light-emitting diodes," Opt. Express **19**(S5), A1135–A1140 (2011).
12. M. C. Tseng, D. S. Wuu, C. L. Chen, H. Y. Lee, Y. C. Lin, and R. H. Horng, "Performance comparison of p-side-up thin-film AlGaInP light emitting diodes with aluminum doped zinc oxide and indium tin oxide transparent conductive layers," Opt. Mater. Express **6**(4), 1349–1357 (2016).
13. R. Olshansky, "Propagation in glass optical waveguides," Rev. Mod. Phys. **51**(2), 341–367 (1979).
14. A. W. Snyder, and J. D. Love, *Optical Waveguide Theory* (Chapman and Hall, 1983), part I.
15. D. Gloge, "Weakly Guiding Fibers," Appl. Opt. **10**(10), 2252–2258 (1971).
16. R. Hauschild and H. Kalt, "Guided modes in ZnO nanorods," Appl. Phys. Lett. **89**(12), 123107 (2006).
17. T. Nobis and M. Grundmann, "Low-order optical whispering-gallery modes in hexagonal nanocavities," Phys. Rev. A **72**(6), 063806 (2005).
18. Y. P. Varshni, "Temperature dependence of the energy gap in semiconductors," Physica **34**(1), 149–154 (1967).

1. Introduction

The high-efficiency light emitter diode (LEDs) of AlGaInP-base quaternary material is currently most potential solid-state light source, with an increasing number of applications in traffic signals, liquid crystal display backlight unit, indoor and outdoor displays, etc [1]. However, a serious obstacle to AlGaInP-base LEDs is the low light extraction efficiency (LEE) due to a considerable absorbing GaAs substrate and Fresnel loss. Fresnel loss is due to the sharp refractive index difference from GaP window layer ($n \approx 3.5$) to air ($n \approx 1$) or epoxy ($n \approx 1.5$). According to the Snell's law, the critical angle in AlGaInP-base LEDs is approximately 16.6° (for air) or 25.4° (for epoxy) due to total internal reflection effect [2]. Therefore, most of the generated photons are confined inside of LEDs and absorbed by LED chip to generate Joule heat. Many processes have been developed in enhancing light extraction efficiency of AlGaInP LEDs for high-brightness. They are change of cavity geometry [3], roughening the emitting surface [4], fabrication of photonic crystal structure [5], etc. Moreover, various thin films which have transparent, electric conductivity and lower refractive index properties were deposited on the GaP layer surface to reduce the gap of refractive index between GaP window layer and packaged material epoxy [6]. The absorbing GaAs substrate was replaced by a thermal conductive silicon substrate via a directly wafer-bonding technique [7] or electroplating Cu substrate [8].

The ZnO nanorods grown by the hydrothermal method have been studied to improve the LEE of LED due to the advantages of low cost, low grown temperature and damage-free process [9,10]. The refractive index of ZnO ($n \sim 2.0$) is between the semiconductor and epoxy ($n = 1.5$). The refractive index of III-Nitride base and III-Phosphide base active layer are approximately 2.5 and 3.5, respectively. Therefore, the ZnO nanorod is a good graduated refractive index material for III-Nitride base and III-Phosphide base LED [11]. Most of the study focus on the ZnO nanorods grown on the III-Nitride base LED to enhance light extraction efficiency. However, the effect of ZnO nanorods structure on the performance of thin film *p*-side up AlGaInP did not be studied. In our previously research [12], we have successfully replaced the ITO by AZO thin film, which directly contacted on the *p*-GaP windows layer for *p*-side-up thin-film AlGaInP LED applications. In this work, the ZnO nanorods are further grown on the AZO thin film by hydrothermal method to further improve the LEE. The performance of *p*-side-up thin-film AlGaInP LEDs with ZnO nanorods are studied in detail.

2. Experimental details

The AlGaInP LED epilayers were grown on *n*-type GaAs substrates by metal-organic chemical vapor deposition. The LED structure consists of a carbon-doped p^+-GaP ohmic contact layer, *p*-GaP:Mg window layer, *p*-cladding AlGaInP, GaInP–AlGaInP MQWs, *n*-cladding AlGaInP, n^+-GaAs contact layer, and GaInP etching stop layer. The AlGaInP LED structure was transferred onto silicon substrate by twice wafer-transfer technique to fabricate high-brightness *p*-side-up thin-film AlGaInP LEDs. The twice wafer-transfer technique procedures have been detailed in our previous studies [7]. The schematic diagram of *p*-side up

Optical Materials EXPRESS

thin film AlGaInP-based LED with ZnO nanorods is shown in Fig. 1. The AZO thin film was deposited on a *p*-side-up thin-film AlGaInP LED with a Zn:Al cycle ratio of 20:1 by using atomic layer deposition (ALD). The deposition temperature and pressure were 200 °C and 0.6 Torr, respectively. Diethylzinc [$Zn(C_2H_5)_2$, DEZn], trimethylaluminum [$Al(CH_3)_3$], and deionized water were used as Zn, Al, and O precursors for depositing the AZO thin film. The growth rate of AZO thin film was 0.14 nm/cycle. The Al was doped into the ZnO film by introducing the Al precursor into the reaction chamber once during all 20 cycles of DEZn injections. Following, the ZnO nanorods were grown on the AZO seed layer through hydrothermal method. The zinc acetate dihydrate ($Zn(CH_3COO)_2{\cdot}2H_2O$, 99.9%) and hexamethylenetetramine (HMTA, $C_6H_{12}N_4$, 99.9% purity) were dissolved in de-ionized water. The molar concentration of hydrothermal nutrition solution was consisted of the equivalent molar concentrations of zinc acetate hydrate and HMTA (i.e., 1:1) in the sealed glass beaker under constant stirring at a temperature of 65°C, 75°C and 85°C. The molar concentrations of hydrothermal nutrition solution were 40 mM and 80 mM, respectively. The diameter and length of ZnO nanorod was measured by high-resolution field emission scanning electron microscopy (FE-SEM). The AlGaInP LED wafer with AZO seed layer was vertically dipped into the hydrothermal nutrition solution. The different diameter and length of ZnO nanorods were obtained by various concentration and growth temperature of hydrothermal nutrition solution. The growth time of ZnO nanorods with different growth parameter was 1 hours. Evaluation of the effect of the ZnO nanorods on the light extraction efficiency of the LED performance is important; the six types of nanorods with different diameters and length were fabricated using the same epilayers. The Ti/Al/Ti/Au (25/2000/50/100 nm) as front grid metal was deposited on top of the transparent conductive layer. The bottom electrode Ti/Au (5/100 nm) was deposited on the rear of Si substrate. Finally, all samples were cut into separated chips with dimensions of 1010 × 1010 μm^2. Ref-LED is *p*-side-up thin-film AlGaInP LED with AZO current spreading layer; ZnO nanorods with different diameters and length were deposited on AZO seed layer of a *p*-side-up thin-film AlGaInP LED for comparison, noted as NR-LED-I ~NR-LED-VI with different growth parameters. All optoelectronic characteristics shown in this research were obtained from the average data measured 50 different samples. In addition, the reproducibility of optoelectronic characteristics is about 90%.

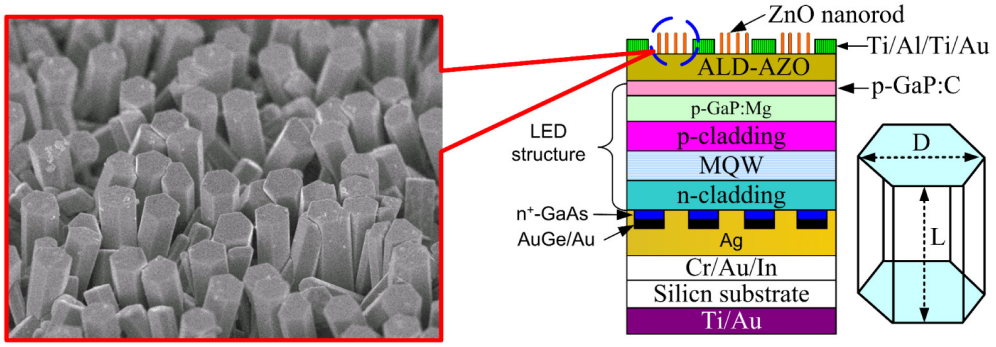

Fig. 1. Schematic diagram of *p*-side up thin film AlGaInP-based LED with ZnO nanorods after twice wafer-transferring technique and symbol description of ZnO nanorod (D: diameter, L: length).

3. Results and discussion

It is necessary to provide a seed layer for the ZnO nanorods grown by hydrothermal method. Here, the AZO thin film deposited on the GaP windows layer was used as a seed layer before ZnO nanorods grown. It is worth mentioning that the AZO is not only the seed layer, but also an ohmic contact layer with the GaP window layer. The ohmic contact characteristics of the AZO thin film with the *p*-GaP:C cap layer is key issue in the performance of the *p*-side-up thin-film AlGaInP LEDs and has been studied in our pervious paper [12].

Optical Materials EXPRESS

By adjusting the precursor concentration and reaction temperature, the different diameter and length of ZnO nanorod structures are shown in Fig. 2 and Fig. 3. Note that the error of measured size is about ± 10 nm. The SEM images of nanorods were grown under different reaction temperature (85°C, 75°C and 65°C) and precursor concentration (40 mM and 80 mM). The structures of the ZnO nanorod exhibit the hexagonal-shape. In the concentration of 80 mM (as shown in Fig. 2), the shape of nanorods becomes from branched-like to particle-like when the reaction temperature decreased from 85°C to 65°C. The distribution density and orientation of ZnO nanorods were significantly affected by different reaction temperature. In the concentration of the 40mM (as shown in Fig. 3), the average diameter of the ZnO nanorods was smaller than that of the concentration of 80 mM. The orientation of ZnO nanorods was grown toward the random direction and uniformly covered the entire surface. The distribution density and orientation of ZnO nanorods presents almost the same and exhibits the hexagonal-shape. The part of ZnO nanorods coalesced to form non-hexagonal structure with relative large size. The growth time and concentration contribute the both volume expansion and length of ZnO nanorods. The growth time was fixed at 1 hour in this study. Therefore, the volume expansion of nanorods was the primarily controlled by concentration of hydrothermal solution and concurrently expanded to laterally to merge with neighboring individual ZnO nanorod, especially in concentration of 80mM with different growth temperature.

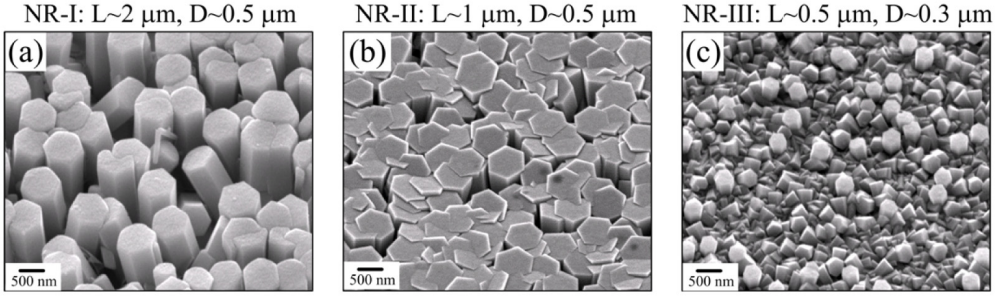

Fig. 2. SEM Images of ZnO nanorods with concentration of 80 mM under different reaction temperature (a) 85°C, (b) 75°C and (c) 65°C.

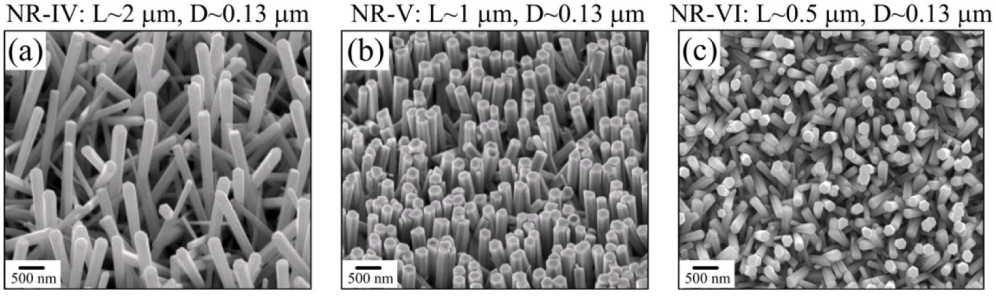

Fig. 3. SEM images of ZnO nanorods with concentration of 40 mM under different reaction temperature (a) 85°C, (b) 75°C and (c) 65°C.

The average length of ZnO nanorods in the same precursor concentration was significantly influenced by reaction temperature. They were estimated to be approximately 2 μm, 1 μm and 0.5 μm for 85°C, 75°C and 65°C, respectively. Obviously, the length of nanorod increases as reaction temperature. Moreover, the average diameter of ZnO nanorods was obtained by adjusting the precursor concentration of 40 mM and 80 mM, which was approximately 0.13 μm and 0.5 μm, respectively. The increment in average diameter of ZnO nanorods was attributed to increase in concentration of Zn^{2+} in the reaction aqueous solution. The lateral growth of ZnO nanorods via the increasing concentration of Zn^{2+} in the hydrothermal

Optical Materials EXPRESS

nutrition aqueous solution was nonlinearly increased. With increase the average diameter of the ZnO nanorods, the distribution density of the ZnO nanorods was increased. The ZnO nanorods coalesced to form large pillar structure in the high concentration hydrothermal nutrition aqueous solution with different reaction temperature.

Notably, the distribution of ZnO nanorods was sparse and oblique in the Fig. 2(c). This could be due to the etching reaction of the ZnO-base material to modify the surface morphology of seed layer at the initial nanorod growth. In this study, the seed layer for ZnO nanorods growth was the AZO thin film. Here, main composition of the AZO was ZnO-base material. The ZnO nanorods grown on modified AZO seed layer surface becomes small and sparse distribution as the growth parameter is high concentration and low reaction temperature. Most of the ZnO nanorods grown on the modified AZO thin film could become oblique. The ZnO nanorods exhibit inclined growth direction and laterally merge with neighboring single ZnO nanorod to from the rough surface. A part of ZnO nanorods were perfect hexagonal shape.

A major concern regarding the ZnO nanorods grown on the AZO thin film contacting the *p*-GaP window layer of the *p*-side-up thin-film AlGaInP LEDs is the I–V characteristics. The forward I–V characteristics of Ref-LED and NR-LED-I to NR-LED-VI are shown in Fig. 4. All LED structures exhibited normal *p–n* diode behaviors at a forward dc bias. At an injection current of 350 mA, the turn-on voltages of Ref-LED and NR-LED-I to NR-LED-VI were 2.41, 2.44, 2.42, 2.42, 2.47, 2.46, and 2.44V, respectively. The turn-on voltage of the Ref-LED was lower than that of the NR-LED-I to NR-LED-VI. Because the AZO thin film covers the whole *p*-GaP layer, the AZO thin film can act as not only an ohmic contact layer but also a current spreading layer when the current is injected from the top contact metal through the AZO thin film to the whole chip. However, partial AZO layer was etched for the nanorods growth and resulted in a little higher voltage. Even though, the forward voltages of LEDs with ZnO nanorods did not significantly be changed. This indicated that ZnO nanorods did not degrade the electrical property of LEDs in the hydrothermal growth process. It also means that the ZnO nanorods with different parameter grown on the AZO thin film are without serious influence on the current spreading ability of LEDs.

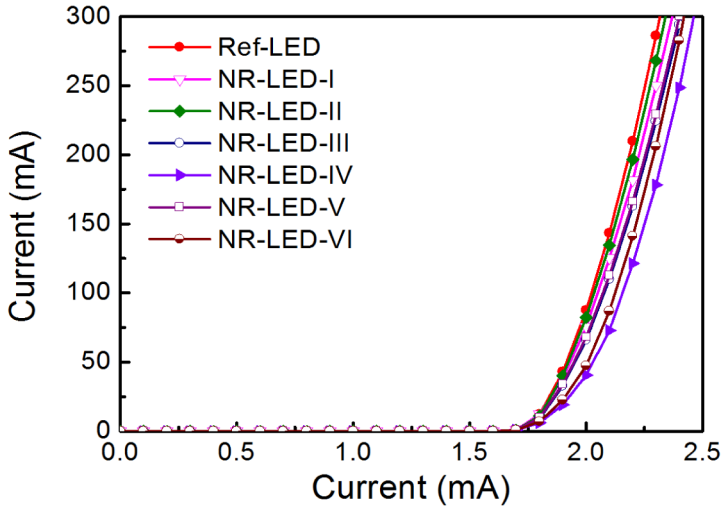

Fig. 4. Forward I-V characteristics for Ref-LED, and NR-LED-I to NR-LED-VI.

The main concerning of LEDs with nanorods structure is the performance of light extraction. Figure 5(a) illustrates the output power characteristics of the LEDs as a function of the injection current at room temperature. According to Fig. 5(a), all LED structures exhibited a linear relationship between the injection current and output power. The output powers of the Ref-LED exhibited stable at high injection currents (>700 mA) because of alleviation of the

Optical Materials EXPRESS

current crowding near the *p*-pad metal. The injected current was more uniform cross the whole chip via AZO thin film to enhance the current spreading, which further improved the output power of the Ref-LED. The output powers of Ref-LED and NR-LED-I to NR-LED-VI were 279, 310, 350, 291, 326, 342, and 368 mW at an injection current of 700 mA, and 373, 412, 470, 392, 438, 452, 490 mW at an injection current of 1000 mA, respectively. The output power characteristics of LED with ZnO nanorods structure were higher than that of the Ref-LED. The output powers of NR-LED-I to NR-LED-VI increased by 11%, 25%, 4%, 17%, 23%, and 32% at an injection current of 700 mA and 10%, 26%, 5%, 17%, 21%, and 31% at an injection current of 1000 mA, respectively, compared with that of the Ref-LED. The improvement in the output power for LED with optimum ZnO nanorods structure was greater than 30% because photons were extracted from the LED structure, further reducing the accumulation of Joule heat. It is worth mentioning that the output power of the NR-VI-LED increased by 32% and 31% at injection current of 700 mA and 1000 mA, respectively. This suggests that the NR-VI-LED can much more effectively extract light from GaP layer to epoxy than the Ref-LED does and keep stability LEE.

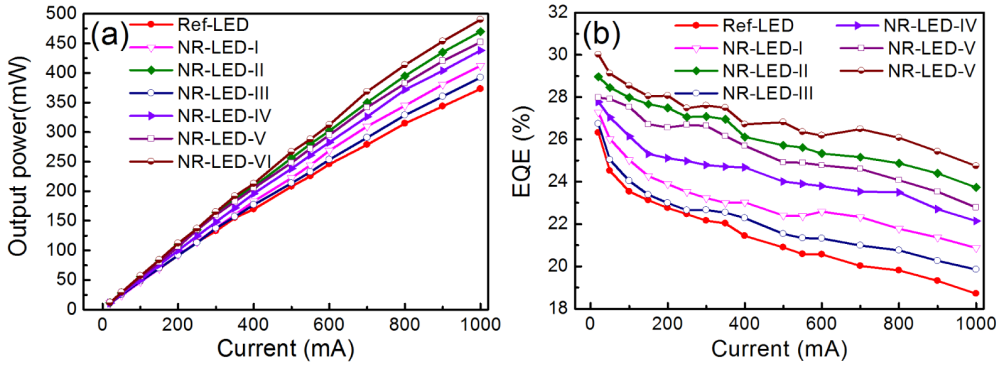

Fig. 5. (a) Output power characteristics, (b) external quantum efficiencies (EQE) for Ref-LED, and NR-LED-I to NR-LED-VI.

The external quantum efficiencies of Ref-LED, and NR-LED-I to NR-LED-VI were 26%, 27%, 29%, 27%, 28%, 28%, and 30% at an injection current of 20 mA, respectively (Fig. 5(b)). In addition, the droop efficiencies of Ref-LED, and NR-LED-I to NR-LED-VI were 29%, 23%, 18%, 26%, 20%, 19%, and 18%, respectively. The droop efficiency (Definition: $[(EQE_{max}-EQE_{min})/EQE_{max}] \times 100\%$) was obviously improved by introducing the AZO thin film and ZnO nanorods structure. The internal quantum efficiency (IQE) is estimated by temperature-dependent photoluminescence (PL). The PL intensity of the emitted light after PL excitation is measured at low temperature (I_{LT}, ~77 K) and room temperature (I_{RT}). The IQE is estimated the ratio of the peak PL intensities ($(I_{RT}/ I_{LT}) \times 100\%$). The IQE of the *p*-side-up AlGaInP LED was 97.62% after PL measurement (not shown). After calculation ($EQE = IQE \times \eta_{extrac}$), the η_{extrac} of Ref-LED, and NR-LED-I to NR-LED-VI were 27%, 28%, 30%, 28%, 29%, 29% and 31% at an injection current of 20 mA, respectively. The light extraction efficiencies of NR-LED-I to NR-LED-VI were improved by 4%, 11%, 4%, 7%, 7%, and 15% compared with the efficiency of Ref-LED at an injection current of 20 mA, respectively.

The output power has been enhanced by AZO thin film due to reduction in the reflective index of GaP. In this study, the ZnO nanorods as additional light extraction layer covering the entire surface of the LED device. More light output of LEDs will be expected, which will further improve the light extraction efficiency. The light extraction efficiency of an LED will be influenced by different nanostructures of ZnO nanorods with different growth parameter. More light will be extracted from ZnO nanorods coupling through propagation in ZnO nanorods to convert waveguide modes into radiation modes. To understand the relevant to light propagation that governs the waveguide effect and increased the output power intensity

Optical Materials EXPRESS

through the ZnO nanorods. The EL peak of an LED device with ZnO nanorods is assumed to be 616 nm, which is used for numerical calculations of mode distribution in the waveguide theory. A schematic of the waveguide ZnO nanorods in this study is depicted in the Fig. 6 as a step index optical fiber. The core region, ZnO nanorods, has greater refractive index (n_1; n_{ZnO}≈2.0) than the cladding region, epoxy (n_2; n_{epoxy} ≈1.5). Because of the large refractive index different at epoxy/ZnO nanorods, the most of the incident light energy could be confined within the core region (ZnO nanorods) until the light escape at the top end of nanorods. The step index waveguide has two different guide modes: single-mode waveguide and multi-mode waveguide condition. The light can be delivered to the end of core with less energy loss when the ZnO nanorod works under single mode condition. Meanwhile, in the multi-mode condition, the light energy can be significantly loss by the intermodal dispersion [13].

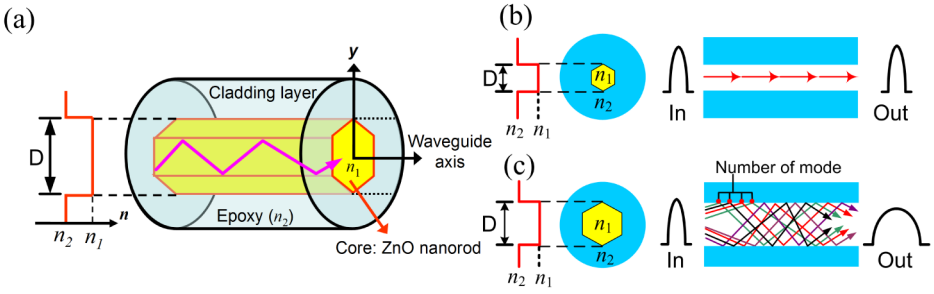

Fig. 6. (a) schematic of the waveguide ZnO nanorod as a step index waveguide optical fiber, (b) the schematic of single-mode step index waveguide, (c) the schematic of multi-mode step index waveguide.

The light wave can be propagated along the ZnO nanorods when the nanorods waveguide mode satisfies waveguide parameter (V) as following equation [14],

$$V = \pi \frac{d}{\lambda} \sqrt{\left(n_{zno}^2 - n_{epoxy}^2\right)} \tag{1}$$

where λ is the wavelength of light (≈616 nm) and d is the diameter of ZnO nanorod. The n_{ZnO} and n_{epoxy} are refractive indices of ZnO nanorod and epoxy, respectively. The single-mode waveguide cut-off diameter corresponds to V = 2.405, the critical diameter of ZnO nanorod at wavelength of 616nm is 0.356 μm. The quantity V is employed to classify fiber operating at single-mode condition (V<2.405) or multi-mode condition (V>2.405). The number of modes means the light path, which propagates in the ZnO nanorods. The average diameter of ZnO nanorods in this study were 0.13 μm, 0.3 μm, and 0.5 μm, respectively. The diameters of 0.13 μm and 0.3 μm can satisfy the single-mode waveguide condition. The large improvement in light output power of LED with the 0.13 μm diameter ZnO nanorods is attributed to propagation of light wave along the ZnO nanorods due to single-mode waveguide effect. But the optical performance of an LED with the 0.3 μm diameter ZnO nanorods shows the minimum improvement, the reason will be discussed later. In addition, the number of modes (M) in the multi-mode condition can be calculated from the following equation [15–17]:

$$M \approx V^2 / 2 \tag{2}$$

The 0.5 μm diameter ZnO nanorods satisfy the multi-mode waveguide condition. Numerous modes can exist within in the core region (calculated number of modes: 6), the 0.5 μm diameter ZnO nanorods propagates light with poor beam quality and lower light intensity compared to the ZnO nanorods operating in single-mode waveguide condition. Therefore, the most of the LED devices with the 0.5 μm diameter ZnO nanorods exhibit lower improvement. In addition, the light propagates in long distance (it is the length of ZnO nanorod in this study) will cause the broadening incident light and reduce the light intensity. Although, the 0.13 μm

Optical Materials EXPRESS

diameter ZnO nanorods is operated in the single-mode waveguide condition, the longer length of ZnO nanorods was cause of the lower output power intensity in the concentration of 80 mM under different reaction temperature. Therefore, the increment in ZnO nanorods length applying to LED device exhibits the LED performance decrease. Most of the LED device with diameter of 0.13 μm ZnO nanorods exhibits the higher output power characteristic than that of the LED device with diameter of 0.5 μm ZnO nanorods.

The performance of the NR-LED-II is the only parameter (with diameter of 0.5 μm) higher than that of the LED with 0.13 μm diameter ZnO nanorods (except NR-LED-VI). Because the structure of NR-II not only shows well aligned and but also exhibits tight squeeze distribution. Most light transmits in the ZnO nanorods and escapes out toward the normal direction with less light intensity loss, although the NR-II was classified to multi-mode waveguide. Therefore, most lights of NR-LED-II focus in the normal direction, which will cause smaller view angle in the radiation pattern. The LED device with 0.3 μm diameter ZnO nanorods (NR-LED-III) shows the minimum improvement, because of most of the ZnO nanorods shows very oblique growth condition and concurrently expanded laterally to merge with neighboring single nanorod. The rough surface was form via coalesced ZnO nanorod. The minority ZnO nanorod exhibits a complete shape and shows the sparse distribution density. Therefore, only less light can be guide in the ZnO nanorods until the light escape out at the top end of ZnO nanorods.

Figure 7 shows the light emission wavelengths of Ref-LED and NR-LED-I to NR-LED-VI. The electroluminescence peaks of Ref-LED, and NR-LED-I to NR-LED-VI were 616, 615, 614, 614, 615, 614 and 615 nm at an injection current of 20 mA, respectively. It is worth mentioning that the Ref-LED and LEDs with different size and density nanorods present almost the same wavelength (614-616 nm) at the low injection current(20 mA). Obviously, strain status in the active layer dose not be changed for different size and density nanorods. Nevertheless, the wavelength red-shifts of Ref-LED and NR-LED-I to NR-LED-VI were approximately 18, 13, 12, 14, 12, 11, and 11 nm at an injection current of 20–1000 mA, respectively. The increase in the wavelength shift was corresponding to junction temperature of the LED [18]. Therefore, the junction temperature of the Ref-LED will higher than those of the NR-LEDs. Base on the results, the various wavelength shifts of NR-LED-I to NR-LED-VI were 11 ~14 nm. The wavelength shift of the NR-LED-III was obviously large than that of the other LED with nanorod structure. Because of the nanorod structure was short and poorly aligned in the NR-LED-III. Most of the light emission was totally reflected and re-absorbed in active layer of the LED structure. Therefore, the accumulation of Joule heat in the NR-LED-III will be increased, which further increase junction temperature of the LED device. The wavelength shifts of LEDs devices with ZnO nanorod (except for NR-LED-III) were 11~12 nm at injection current of 20~1000 mA. This suggests that LEDs devices with ZnO nanorods not only enhance light extraction but also obtain stability junction temperature of LEDs devices to provide batter thermal stability.

Optical Materials EXPRESS

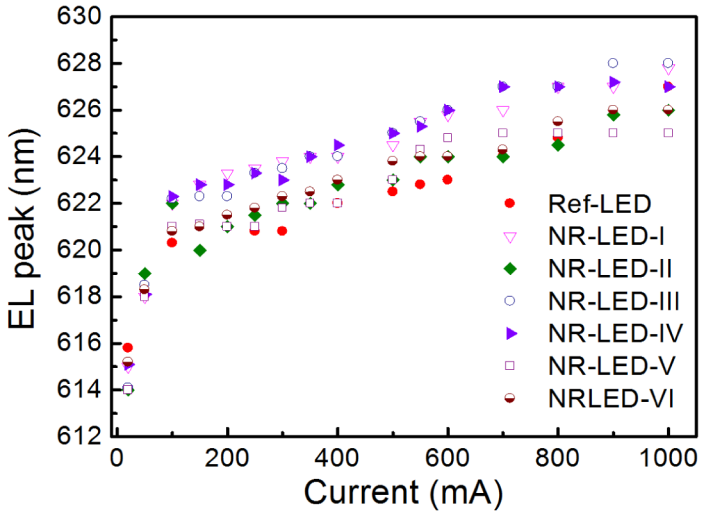

Fig. 7. Emission wavelengths of Ref-LED, and NR-LED-I to NR-LED-VI with different injection current.

The far-field radiation patterns of Ref-LED, and NR-LED-I to NR-LED-VI at an injection current of 350 mA was illustrated in Fig. 8. The output intensities of the LEDs with ZnO nanorods were higher than that of Ref-LED in the full angles. The sharp refractive index between GaP layer (n ≈3.5) and epoxy layer (n ≈1.5) was reduced by AZO thin film (n ≈2.0). In addition, the light extraction efficiency of AZO thin film (n ≈2.0 at a wavelength of 610 nm) was improved due to the reduction of the sharp refractive index difference between the GaP layer to epoxy layer to minimize the total internal reflection effect. The light extraction efficiency of the LEDs was further improved by ZnO nanorods. Therefore, more light can escape from the surface of the LED, preventing the trapping most of photons inside the LED in a guided mode. Particularly, the highest intensity enhancement was obtained along the normal direction and decreased gradually as the emission angle increased. The intensity in the normal direction (0° direction) are consistent with the optoelectronic performance of the LEDs with the AZO thin film and the ZnO nanorods. The viewing angles of Ref-LED, and NR-LED-I to NR-LED-VI were 123°, 128°, 126°, 128°, 126°, 128°, and 122°, respectively. More light was extracted from the surfaces of LED with the optimum ZnO nanorod structure (NR-VI) than that of the Ref-LED, thus reducing the guiding mode light and finally resulting in a narrower viewing angle. The number of viewing angle in LED with nanorods structure is influenced by different morphology of nanorods. The narrow view angle means that most of the lights escaped through the top of the ZnO nanorods to force the light emission toward the normal direction. It is worth mentioning that the some viewing angle of the LED with ZnO nanorod structure was large than that of the Ref-LED. Because of the oblique ZnO nanorods, a part-light was extracted toward the random direction. Therefore, most of the light significantly increased intensity in the normal direction can be reasonably explained by the light emission escaping through the top of oblique ZnO nanorods structure to broad radiation pattern.

Optical Materials EXPRESS

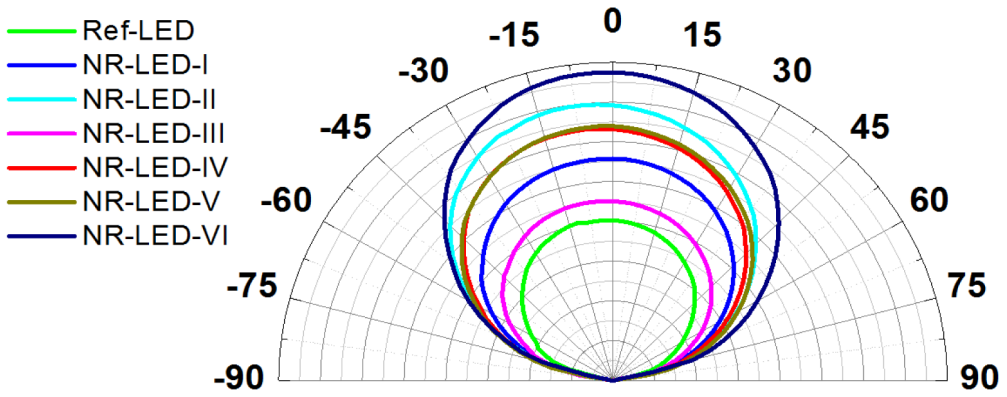

Fig. 8. Far-field radiation patterns of Ref-LED, and NR-LED-I to NR-LED-VI at the injection current of 350 mA.

4. Conclusion

This article reports on ZnO nanorods grown on the *p*-side-up thin-film AlGaInP LEDs to improve the light extraction efficiency. Compared with the Ref-LED, applying ZnO nanorod structures on *p*-side-up thin-film AlGaInP LEDs (NR-LED-I to NR-LED-VI) improved the light extraction efficiency. The output power characteristics of *p*-side-up thin-film AlGaInP LEDs were varied with the different diameter and length of ZnO nanorods. The improvement in output power characteristic of *p*-side-up thin-film AlGaInP LEDs with optimum ZnO nanorod structure were 32% and 31% as compared with the Ref-LED in the injection current of 700 and 1000mA, respectively. The ZnO nanorods grown on the LED device provide the stability improvement. The large enhancement of the optical output power in LED device was attributed to the light propagation through the inclined ZnO nanorods with waveguide effect. Furthermore, the broad radiation patterns of *p*-side-up thin-film AlGaInP LEDs with ZnO nanorod structures were also improved through the inclined ZnO nanorods to force the light emission toward the normal direction and enhance the light extraction. The morphology of ZnO nanorods was the main factor to influence the light extraction efficiency and radiation patterns for LED device. Therefore, the ZnO nanorods using hydrothermal method were potentially useful in AlGaInP LED applications and can reduce their manufacturing cost.

Funding

Ministry of Science and Technology (MOST 102-2221-E-005-071-MY3 and 104-2221-E-005-031-MY3); HsinChu Science Park and Southern Taiwan Science Park (101A08, 102CE06, and 105CE01).